

Novel and potent cyclic cyanamide-based cathepsin K inhibitors

David N. Deaton,^{a,*} Anne M. Hassell,^b Robert B. McFadyen,^a
Aaron B. Miller,^b Larry R. Miller,^c Lisa M. Shewchuk,^b Francis X. Tavares,^a
Derril H. Willard, Jr.,^{d,*} and Lois L. Wright^e

^aDepartment of Medicinal Chemistry, GlaxoSmithKline, Research Triangle Park, NC 27709, USA

^bDiscovery Research Computational, Analytical, and Structural Sciences, GlaxoSmithKline, Research Triangle Park, NC 27709, USA

^cDepartment of Molecular Pharmacology, GlaxoSmithKline, Research Triangle Park, NC 27709, USA

^dDepartment of Gene Expression and Protein Purification, GlaxoSmithKline, Research Triangle Park, NC 27709, USA

^eDiscovery Research Biology, GlaxoSmithKline, Research Triangle Park, NC 27709, USA

Received 31 January 2005; revised 9 February 2005; accepted 11 February 2005

Abstract—Starting from a PDE IV inhibitor hit derived from high throughput screening of the compound collection, a key pyrrolidine cyanamide pharmacophore was identified. Modifications of the pyrrolidine ring produced enhancements in cathepsin K inhibition. An X-ray co-crystal structure of a cyanamide with cathepsin K confirmed the mode of inhibition.

© 2005 Elsevier Ltd. All rights reserved.

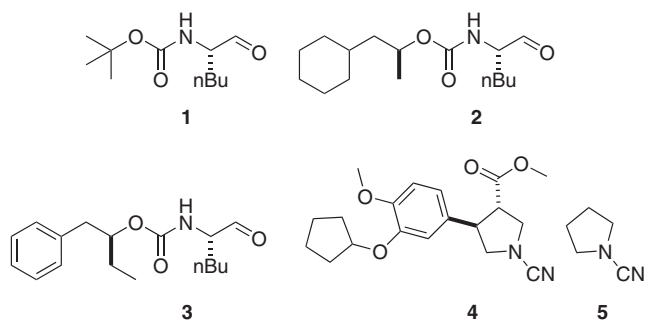
Skeletal fragility, resulting from the loss of bone mineral density and integrity, is the leading cause of non-traumatic fracture.¹ Typically, this phenotype results from an imbalance in the normally tightly coupled processes of bone formation and bone resorption that maintain skeletal homeostasis. Bone is resorbed by osteoclasts, which secrete protons and proteases that degrade the mineral and protein components of bone. The cysteine protease cathepsin K is highly expressed in osteoclasts and rapidly hydrolyzes type I collagen, the major component of bone matrix, as a complex with glycosaminoglycans.² A rare human deficiency in cathepsin K is the cause of pycnodysostosis, an autosomal recessive trait characterized by short stature, abnormal bone, and tooth development, increased bone mineral density, and increased bone fragility.³ In light of the key role played by cathepsin K in bone resorption, pharmaceutical companies have pursued the development of cathepsin K inhibitors for the treatment of osteoporosis,⁴ and small molecule inhibitors of cathepsin K have proven efficacious in attenuating bone resorption in animal models of osteoporosis.⁵

As part of a larger program to develop novel cathepsin K inhibitors, researchers from these laboratories recently reported the discovery of aldehyde-based cathepsin K inhibitors.^{6,7} Starting from a focused screening hit, Boc-Nle-H **1** (IC₅₀ = 51 nM), potent inhibitors like **2** (IC₅₀ = 2.7 nM) and **3** (IC₅₀ = 0.13 nM) were developed by optimizing P²–P³ substituents. In addition to this focused screen approach to hit discovery, a high throughput screen of the GlaxoWellcome compound collection was also employed, resulting in the identification of the PDE IV inhibitor **4**⁸ as a reasonably active cathepsin K inhibitor (IC₅₀ = 430 nM).⁹ This cyanamide-containing compound proved to be a reversible and substrate-competitive inhibitor. Surmising that the cyanamide was acting as an active site electrophile for the ²⁵Cys thiol, the commercially available truncated N-pyrrolidinecarbonitrile **5** (IC₅₀ = 2100 nM) was also tested and found to be a micromolar inhibitor of cathepsin K. Pyrrolidine **5** was chosen as a key pharmacophore for further optimization with the goal of appending substituents to the α- or β-position to interact with the S² subsite, the deepest, most pronounced hydrophobic binding pocket of the cathepsin K active site. Subsequent to this work being completed, Merck/Celera researchers also reported the discovery of cyanamide-based cathepsin K inhibitors from a HTS hit.^{10,11} The results of efforts to design and prepare potent cathepsin K inhibitors derived from cyanamide **5** are detailed in this report.

Keywords: Cathepsin K; Cyanamide; Cysteine protease inhibitor; Warhead.

* Corresponding author. Tel.: +1 919 483 6270; fax: +1 919 315 0430;
e-mail: david.n.deaton@gsk.com

*Deceased.

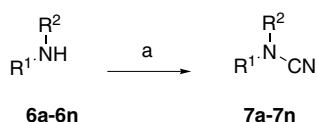


The cyanamides **7a–n** were synthesized from the corresponding amines **6a–n** as shown in **Scheme 1**. Treatment of the amine with cyanogen bromide in the presence of a base produced the desired cyanamides in reasonable yields.

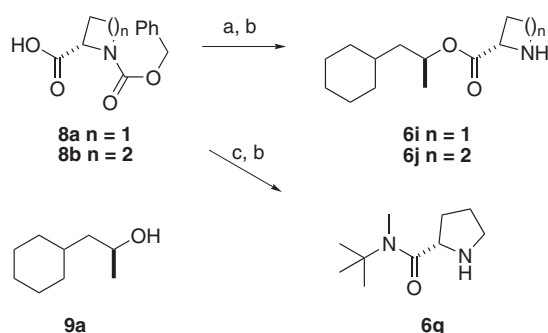
The amines **6a–o** utilized for this coupling were either commercially available (**6a–d**), known in the literature (**6e,f**, and **h**),^{12–14} or synthesized as depicted in **Schemes 2–4** (**6g, i–n**).

As shown in **Scheme 2**, the known acid **8a**¹⁵ and commercially available acid **8b** were converted to esters of known alcohol **9a**⁷ via the method of Fischer. Then the carbamates were cleaved to provide the amines **6i** and **j**. The amine **6g** was also obtained from **8b**. Reaction of its acid chloride, obtained from treatment of **8b** with oxalyl chloride, with *tert*-butylmethylamine in the presence of triethylamine afforded the amide. Catalytic hydrogenation of the benzyl carbamate as before yielded the amine **6g**.

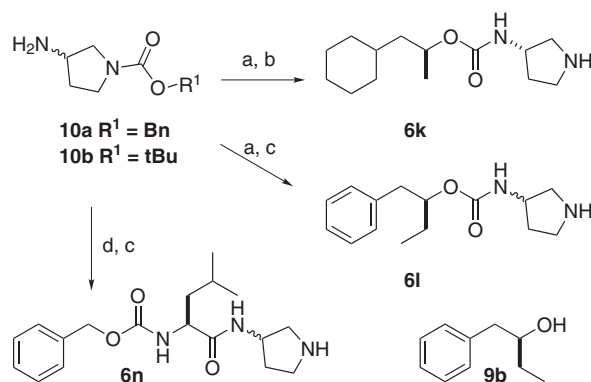
The amine **6k** was synthesized from the commercially available amine **10a** as illustrated in **Scheme 3**. Alcohol



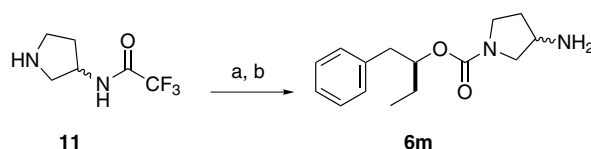
Scheme 1. Reagents and conditions: (a) BrCN, K₂CO₃, MeCN, 40–78%.



Scheme 2. Reagents and conditions: (a) **8a** or **b**, **9a**, TsOH, PhH, ↑↓, 61–93%; (b) H₂/Pd–C, MeOH, 77–97%; (c) **8b**, (COCl)₂, PhMe, *t*-BuNHMe, NEt₃, CH₂Cl₂, 83%.



Scheme 3. Reagents and conditions: (a) **9a** or **9b**, 1.93 M COCl₂ in PhMe, pyridine, CH₂Cl₂, –20 °C to rt; **10a** or **10b**, *i*-Pr₂NEt, THF, 59–88%; (b) H₂/Pd–C, MeOH, 98%; (c) HCl, EtOAc, 99%; (d) Cbz–Leu, EDC, HOBT, NMM, 71%.



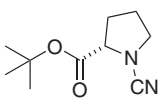
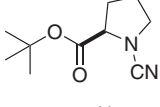
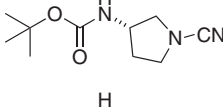
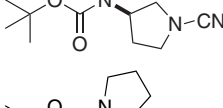
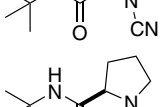
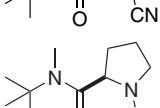
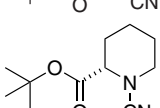
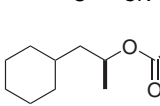
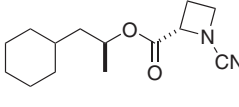
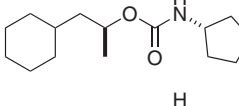
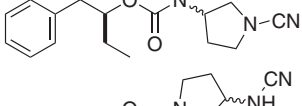
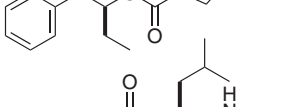
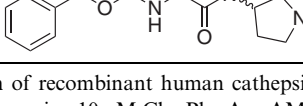
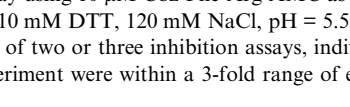
Scheme 4. Reagents and conditions: (a) **9b**, 1.93 M COCl₂ in PhMe, pyridine, CH₂Cl₂, –20 °C to rt; **11**, *i*-Pr₂NEt, THF, 95%; (b) K₂CO₃, MeOH, H₂O, 89%.

9a was converted to its corresponding chloroformate with phosgene, and then coupled to the amine **10a** to give a bis-carbamate. Subsequent hydrolysis of the benzyl carbamate afforded amine **6k**. The amine **6l** was synthesized from the commercially available amine **10b**. As before, conversion of known alcohol **9b**⁷ to its chloroformate and coupling to amine **10b** provided the bis-carbamate. Then, the cyclic amine was deprotected under acidic conditions to provide amine **6l**. Furthermore, amine **10b** was coupled to commercially available cbz-protected leucine via a carbodiimide method to give the amide. Acid catalyzed deprotection of the cyclic amine, as before, provided the amine **6n**.

The reversed pyrrolidine amine **6m** was synthesized as shown in **Scheme 4**. Coupling of the chloroformate derived from alcohol **9b** with the commercially available amine **11** afforded the carbamate. Then, base catalyzed hydrolysis of the trifluoromethyl acetamide provided amine **6m**.

Because the *tert*-butyl P² moiety had provided reasonable potency to aldehyde inhibitor **1**, it was appended to the α- and β-positions of cyanamide **5** to provide the cyanamides **7a–d**. As shown in **Table 1**, the α-series (*S*)-proline derived cyanamide **7a** (IC₅₀ = 60 nM) was 35-fold more potent than the starting cyanamide **5** (IC₅₀ = 2100 nM). Its (*R*)-proline derived enantiomer **7b** (IC₅₀ = 300 nM) was also more potent than analog **5**, but 5-fold less potent than the (*S*)-enantiomer **7a**, suggesting that the inhibitor interacts with the enzyme in a stereospecific manner. Gratifyingly, the β-series (*S*)-cyanamide **7c** (IC₅₀ = 81 nM) was equipotent with the

Table 1. Inhibition of human cathepsin K

#	Inhibitor	IC ₅₀ nM ^a
7a		60
7b		300
7c		81
7d		200
7e		380
7f		8100
7g		>13,000
7h		>13,000
7i		1.8
7j		0.048
7k		12
7l		8.9
7m		200
7n		19

^a Inhibition of recombinant human cathepsin K activity in a fluorescence assay using 10 μM Cbz-Phe-Arg-AMC as substrate in 100 mM NaOAc, 10 mM DTT, 120 mM NaCl, pH = 5.5. The IC₅₀ values are the mean of two or three inhibition assays, individual data points in each experiment were within a 3-fold range of each other.

α-series analog **7a**. Interestingly, the β-series (*R*)-enantiomer **7d** (IC₅₀ = 200 nM) exhibited an inhibitory potency versus cathepsin K not statistically different from

that of **7c**. Apparently, the effect of the stereocenter in the β-position is much smaller than the α-position.

To further explore the influence of the stereocenter adjacent to the pyrrolidine nitrogen, analog **7e** was synthesized, in which replacement of the carbon atom with nitrogen places the presumed P² substituent more in plane with the pyrrolidine ring due to the sp² character of the C–N carbamate bond. This change resulted in a cathepsin K inhibitor that was equipotent with (*R*)-proline derived analog **7b**, confirming the importance of the stereocenter. Since amides are chemically more robust than esters, the amides **7f** and **g** were prepared. Unfortunately, the *tert*-butyl amide **7f** (IC₅₀ = 8100 nM) was >100-fold less active than the ester **7a**, and the *N*-methyl analog **7g** exhibited no inhibition at concentrations up to 13,000 nM.

Desiring to explore if the P²–P³ SAR from the aldehyde-based inhibitors could be further transferred to the cyanamide series, the P²–P³ substituent from aldehyde **2** was incorporated into cyanamide **5** to provide cyanamide **7i** (IC₅₀ = 1.8 nM). The addition of a P³ substituent resulted in a 30-fold boost in inhibitory activity versus cathepsin K. A comparable 18-fold increase was previously realized in the aldehyde inhibitors.⁷

Changing the size of the cyanamide ring should alter the position of the P²–P³ moiety relative to the cyanamide warhead, possibly allowing more favorable interaction with the S² or S³ subsites. To explore this hypothesis, piperidine analog **7h** and azetidine analog **7j** were synthesized. Whereas the piperidine **7h** was completely inactive at concentrations up to 13,000 nM, a greater than 200-fold reduction in potency from **7a**,¹⁶ a comparison of the azetidine **7j** (IC₅₀ = 0.048 nM) with **7i** (IC₅₀ = 1.8 nM) reveals that the four-membered ring is optimal for inhibitory activity versus cathepsin K. Analog **7j** is >30-fold more active than **7i**. Independently, Merck/Celera researchers have also disclosed that the *N*-azetidincarbonitrile warhead is a more active cathepsin K inhibitor than the five-membered *N*-pyrrolidincarbonitrile electrophile.¹⁰ They attribute the increased potency of the four-membered analog to increased reactivity of the azetidincarbonitrile warhead, supporting this assertion with data showing a loss of cathepsin K inhibitory potency of the azetidincarbonitrile relative to the pyrrolidincarbonitrile in the presence of added glutathione at pH = 7.0. Since the basicity of the parent cyclic amines are essentially identical (azetidine p*K*_{BH+} = 11.29, pyrrolidine p*K*_{BH+} = 11.27),¹⁷ the increased reactivity of the azetidine-derived inhibitors must arise from reduced steric impediments to nucleophilic attack as opposed to any electronic effect.

Incorporation of P²–P³ aldehyde potency enhancing groups⁷ at the β-position of the parent cyanamide **5** also produced significant enhancements in inhibitory activity. As shown in Table 1, the P²–P³ analog **7k** (IC₅₀ = 12 nM) was 6-fold more active than the corresponding *tert*-butyl analog **7c** (IC₅₀ = 81 nM), although, less potent than the corresponding α-series analog **7i** (IC₅₀ = 1.8 nM). An attempt to further improve activity

in the β -series, by incorporating the more potent P^2 - P^3 substituent⁷ from aldehyde **3** was not successful, the cyanamide **7i** ($IC_{50} = 8.9$ nM) not being significantly more active than **7k**. Reversal of the substituents on the 3-aminopyrrolidine as in analog **7m** ($IC_{50} = 200$ nM) resulted in a ~ 10 -fold loss in activity.

As shown in Table 2, these analogs exhibit moderate selectivity versus the closely related endopeptidase cathepsin L with selectivity ranging from 6- to 70-fold. In contrast, these cyanamides are more selective versus the exopeptidases cathepsin B (B/K = 56–500) and cathepsin H (H/K = 320–830). These cyanamides were not tested versus cathepsin S, another closely related endopeptidase.

In order to better understand the mechanism of action of these reversible inhibitors, an X-ray co-crystal structure of cathepsin K with the leucine-derived inhibitor **7n** ($IC_{50} = 19$ nM) was solved. This is the first published X-ray co-crystal structure of an inhibitor containing a cyanamide warhead, and the active site is shown in Figure 1. The cyanamide moiety of the inhibitor and the active site ²⁵Cys of the enzyme form a covalent isothioureia intermediate, consistent with the reversible nature of these inhibitors. This structure confirms the ¹³C NMR experiments of the Merck researchers with their cyanamide-based inhibitors and papain.¹⁰ This mechanism of inhibition is similar to the reaction of cysteine proteases with nitriles to form thioimidate esters. The nitrogen of the carbon–nitrogen double bond points into the oxy-anion hole, and is stabilized by hydrogen bonds to the side chain carbonyl of ¹⁹Gln and the backbone NH of ²⁵Cys. One additional hydrogen bond between the peptide backbone recognition site of the enzyme and the amide carbonyl further stabilizes the inhibitor. Thus, the amide carbonyl accepts a hydrogen bond from the backbone NH of ⁶⁶Gly.

Besides these hydrogen bond stabilizing interactions with the protein, the P^2 isobutyl forms lipophilic interactions with the S^2 pocket composed of ⁶⁷Tyr, ⁶⁸Met, ¹³⁴Ala, ¹⁶³Ala, and ²⁰⁹Leu. Moreover, the P^3 phenyl interacts with the S^3 subsite. No interaction is real-

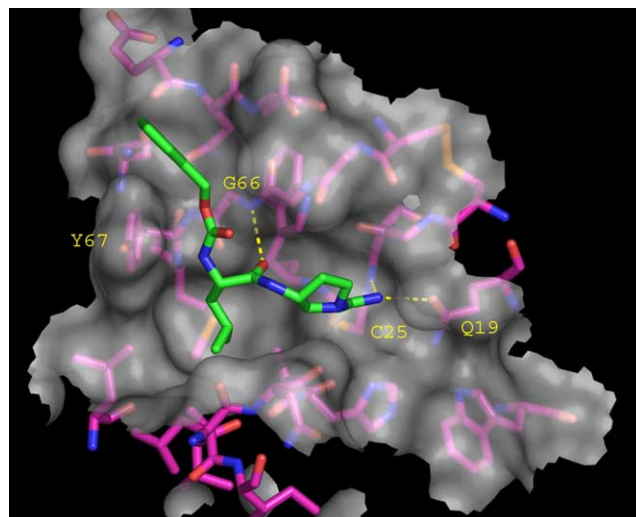


Figure 1. Active site of the X-ray co-crystal structure of compound **7n** complexed with cathepsin K. The cathepsin K carbons are colored magenta with inhibitor **7n** carbons colored green. The semi-transparent white surface represents the molecular surface, while hydrogen bonds are depicted as yellow dashed lines. The coordinates have been deposited in the Brookhaven Protein Data Bank, accession number 1YK7. This figure was generated using PYMOL version 0.97 (Delano Scientific, www.pymol.org).

ized with the S^1 wall formed from ²³Gly, ²⁴Ser, ⁶⁴Gly, and ⁶⁵Gly. Further substitution of the pyrrolidine ring might provide hydrophobic interactions with the S^1 subsite.

In summary, starting from a high throughput screening hit **4**, a key pharmacophore **5** was identified. Addition of a P^2 group to the pyrrolidine led to a >10 -fold increase in potency as in analog **7a**. Subsequent elaboration with P^2 - P^3 moieties derived from aldehyde-based cathepsin K inhibitors produced further enhancements of inhibitory activity as exemplified by analogs **7i** and **k**. Further manipulation of the cyanamide ring size resulted in the discovery of the picomolar cathepsin K inhibitor **7j**. These inhibitors exhibit modest selectivity versus other cathepsin endopeptidases, but their high potency argues for further work to enhance selectivity and other drug properties.

Table 2. Cathepsin B, H, and L inhibition and selectivity

#	Cat K IC_{50} nM	Cat B IC_{50} nM ^a	Cat H IC_{50} nM ^b	Cat L IC_{50} nM ^c
7i	1.8	310	580	130
7j	0.048	2.4	40	0.71
7k	12	680	8300	81

^a Inhibition of recombinant human cathepsin B activity in a fluorescence assay using 10 μ M Cbz-Phe-Arg-AMC as substrate in 100 mM NaOAc, 10 mM DTT, 120 mM NaCl, pH = 5.5. The IC_{50} values are the mean of two or three inhibition assays, individual data points in each experiment were within a 2-fold range of each other.

^b Inhibition of recombinant human cathepsin H activity in a fluorescence assay using 50 μ M L-Arg- β -naphthalamide as substrate in 100 mM NaOAc, 10 mM DTT, 120 mM NaCl, pH = 5.5.

^c Inhibition of recombinant human cathepsin L activity in a fluorescence assay using 5 μ M Cbz-Phe-Arg-AMC as substrate in 100 mM NaOAc, 10 mM DTT, 120 mM NaCl, pH = 5.5.

References and notes

- Einhorn, T. A. In *Osteoporosis*; Marcus, R., Feldman, D., Kelsey, J., Eds.; Academic: San Diego, CA, 1996; p 3.
- Li, Z.; Hou, W.-S.; Escalante-Torres, C. R.; Gelb, B. D.; Bromme, D. *J. Biol. Chem.* **2002**, *277*, 28669.
- Gelb, B. D.; Shi, G.-P.; Chapman, H. A.; Desnick, R. J. *Science* **1996**, *273*, 1236.
- Deaton, D. N.; Kumar, S. *Prog. Med. Chem.* **2004**, *42*, 245.
- Stroup, G. B.; Lark, M. W.; Veber, D. F.; Bhattacharyya, A.; Blake, S.; Dare, L. C.; Erhard, K. F.; Hoffman, S. J.; James, I. E.; Marquis, R. W.; Ru, Y.; Vasko-Moser, J. A.; Smith, B. R.; Tomaszek, T.; Gowen, M. *J. Bone Miner. Res.* **2001**, *16*, 1739.
- Catalano, J. G.; Deaton, D. N.; Furfine, E. S.; Hassell, A. M.; McFadyen, R. B.; Miller, A. B.; Miller, L. R.;

- Shewchuk, L. M.; Willard, D. H.; Wright, L. L. *Bioorg. Med. Chem. Lett.* **2004**, *14*, 275.
7. Boros, E. E.; Deaton, D. N.; Hassell, A. M.; McFadyen, R. B.; Miller, A. B.; Miller, L. R.; Paulick, M. G.; Shewchuk, L. M.; Thompson, J. B.; Willard, D. H.; Wright, L. L. *Bioorg. Med. Chem. Lett.* **2004**, *14*, 3425.
 8. Feldman, P. L.; Brackeen, M. F.; Cowan, D. J.; Marron, B. E.; Schoenen, F. J.; Stafford, J. A.; Suh, E. M.; Domanico, P. L.; Rose, D.; Leesnitzer, M. A.; Brawley, E. S.; Strickland, A. B.; Verghese, M. W.; Connolly, K. M.; Bateman-Fite, R.; Noel, L. S.; Sekut, L.; Stimpson, S. A. *J. Med. Chem.* **1995**, *38*, 1505.
 9. Barrett, D. G.; Clay, W. C.; Deaton, D. N.; Hassell, A. M.; Hoffman, C. R.; Jurgensen, C. H.; Long, S. T.; McFadyen, R. B.; Miller, A. B.; Miller, L. R.; Payne, J. A.; Shewchuk, L. M.; Tavares, F. X.; Wells-Knecht, K. J.; Willard, D. H., Jr.; Wright, L. L. In *Third International Conference on Cysteine Proteinases and their Inhibitors*; Dolinar, M., Turk, B., Turk, V., Eds.; Garamond d. o. o., Ljubljana, Slovenia: Portoroz, Slovenia, 2002; p 95.
 10. Falgueyret, J.-P.; Oballa, R. M.; Okamoto, O.; Wesolowski, G.; Aubin, Y.; Rydzewski, R. M.; Prasit, P.; Riendeau, D.; Rodan, S. B.; Percival, M. D. *J. Med. Chem.* **2001**, *44*, 94.
 11. Rydzewski, R. M.; Bryant, C.; Oballa, R.; Wesolowski, G.; Rodan, S. B.; Bass, K. E.; Wong, D. H. *Bioorg. Med. Chem.* **2002**, *10*, 3277.
 12. Dutta, A. S.; Morley, J. S. *J. Chem. Soc., Perkin Trans. 1* **1975**, 1712.
 13. O'Neil, I. A.; Miller, N. D.; Barkley, J. V.; Low, C. M. R.; Kalindjian, S. B. *Synlett* **1995**, 619.
 14. Egbertson, M.; Danishefsky, S. J. *J. Org. Chem.* **1989**, *54*, 11.
 15. Matsuura, F.; Hamada, Y.; Shioiri, T. *Tetrahedron* **1993**, *49*, 8211.
 16. A simpler analog containing no P² moiety, commercially available N-piperidinecarbonitrile, had also been inactive at 10,000 nM in the high throughput screen of the GlaxoWellcome compound collection.
 17. Ohwada, T.; Hirao, H.; Ogawa, A. *J. Org. Chem.* **2004**, *69*, 7486.